BIOLOGICAL BEHAVIOUR OF CHITOSAN ELECTROSPUN NANOFIBROUS MEMBRANES AFTER DIFFERENT NEUTRALISATION METHODS

Viktoriia Korniienko[1, a, *], Yevheniia Husak[1,2, b], Anna Yanovska[1, c], Şahin Altundal[3], Kateryna Diedkova[1], Yevhen Samokhin[1], Yuliia Varava[1], Viktoriia Holubnycha[1, d], Roman Viter[3, e], Maksym Pogorielov[1,3, f]

[1] Biomedical Research Center, Sumy State University, R.-Korsakova, 2, 40007, Sumy, Ukraine
[a] - ORCID: 0000-0002-5144-2138; [b] - ORCID: 0000-0002-2217-3717;
[c] - ORCID: 0000-0001-8040-7457; [d] - ORCID: 0000-0002-1241-2550;
[f] - ORCID: 0000-0001-9372-7791 ;
[2] Faculty of Chemistry, Silesian University of Technology, 44-100 Gliwice, Poland
[3] Institute of Atomic Physics and Spectroscopy, University of Latvia, Jelgavas iela 3, Riga, LV-1004, Latvia
[e] - ORCID: 0000-0002-9996-041X

** corresponding author: vicorn77g@gmail.com*

Abstract

Chitosan electrospun nanofibres were synthesised in two different trifluoroacetic acid (TFA)/dichloromethane (DCM) solvent ratios and then neutralised in aqueous and ethanol sodium-based solutions (NaOH and Na2CO3) to produce insoluble materials with enhanced biological properties for regenerative and tissue engineering applications. Structural, electronic, and optical properties and the swelling capacity of the prepared nanofibre membrane were studied by scanning electron microscopy, Fourier-transform infrared spectroscopy, and photoluminescence. Cell viability (with the U2OS cell line) and antibacterial properties (against Staphylococcus aureus and Escherichia coli) assays were used to assess the biomedical potential of the neutralised chitosan nanofibrous membranes. A 7:3 TFA/DCM ratio allows for an elaborate nanofibrous membrane with a more uniform fibre size distribution. Neutralisation in aqueous NaOH only maintains a partial fibrous structure. At the same time, neutralisation in NaOH ethanol-water maintains the structure during 1 month of degradation in phosphate-buffered saline and distilled water. All membranes demonstrate high biocompatibility, but neutralisation in ethanol solutions affects cell proliferation on materials made with 9:1 TFA/DCM. The prepared nanofibrous mats could constrain the growth of both gram-positive and gram-negative microorganisms, but 7:3 TFA/DCM membranes inhibited bacterial growth more efficiently. Based on structural, degradation, and biological properties, 7:3 TFA/DCM chitosan nanofibrous membranes neutralised by 70% ethanol/30% aqueous NaOH exhibit potential for biomedical and tissue engineering applications.

Keywords: *chitosan; nanofibres; electrospinning; neutralisation; antibacterial; biocompatibility*

Received: 28.02.2022
Accepted: 18.05.2022

1. Introduction

Polymeric nanofibres are essential materials for biomedical engineering due to their biocompatibility, high surface area, microporosity, and tunable fibre size (length and diameters) [1]. Polymeric nanofibres are often used as active components in medical applications [2], such as tissue engineering [3], drug delivery [4, 5], and skin patches [2], among others. Electrospinning techniques are the most appropriate and convenient approaches to fabricate nanofibres with high specific surface-to-volume ratios, suitable porosity, and a controllable pore size [6]. They have broad potential applications for filtration, bioseparation, biosensing, crop protection, bioremediation, anti-counterfeiting, wound dressings and scaffolds for tissue engineering, sensing applications, controlled drug delivery, reinforcement composites, and micro/nano-electro-mechanical systems [7-10].

Among different biocompatible polymers (collagen, polyvinyl alcohol [PVA], polyethylene oxide [PEO], gelatine, etc.), chitosan (Ch) is the one with the most tailored functional properties [6] and the additional antibacterial activities [11]. Ch electrospun scaffolds have been used for various applications in the biomedical field, such as drug-release systems, bone tissue regeneration, and to heal skin injuries, because they promote additional haemostasis, liquid absorption, cell respiration, and gas permeation [4, 5, 12, 13]. Ch nanofibrous materials support cell migration and proliferation and diminish bacterial contamination [6].

Nanofibre Ch membranes mimic the native extracellular matrix. However, the high viscosity, rigid crystalline structure, and swelling behaviour of Ch membranes in an aqueous medium limit their biomedical applications [14, 15]. Electrospinning Ch-based membranes has some challenges: the selection of solution concentrations and solvents, the parameters of electrospinning deposition, and fibre drying and post-treatment methods.

Applying different solvents and additional post-treatment can provide optimal solutions for nanofibrous membranes with predictable properties. Thus, a combination of solvents is required to improve the low conductivity of a Ch solution. Trifluoroacetic acid (TFA) and dichloromethane (DCM) solvents could improve the homogeneity of the electrospun Ch fibre because the amino groups of the Ch can form salts with the TFA that destroys the interactions between Ch molecules, assisting the electrospinning process [16]. As-spun Ch membranes fabricated from TFA with or without DCM are limited due to loss of fibrous structure or complete membrane dissolution after direct contact with neutral or weak essential aqueous solutions [17]. Indeed, NH_3^+ and CF_3COO^- salt residues formed after Ch dissolves are highly soluble in TFA [17]. Different neutralisation methods have been suggested to maintain the solidity of Ch membranes and to make them insoluble in aqueous media. With this aim, researchers have neutralised Ch fibre membranes in a vapor chamber with 99% ethanol for 72 h at 40°C [18]. Huang *et al.* [19] discussed the effect of absolute ethanol as a neutralising agent for Ch nanofibres.

Based on previous data, adding ethanol to water solutions could lead to fast solvent evaporation with more effective fibre neutralisation. Another reason for adding ethanol is that the amino groups of Ch films neutralised in aqueous sodium hydroxide (NaOH) or NaOH/ethanol are mainly un-protonated because NaOH is a strong alkali: it can react with acids completely. On the other hand, Ch acetate is hydrolysed when treated with ethanol without NaOH. The generated acetic acid molecules are diffused in the ethanol solution and are removed [20]. So, ethanol leads to the fast removal of solvent from membranes.

Sangsanoh *et al.* [21] reported that Ch nanofibres could be neutralised with aqueous NaOH and sodium carbonate (Na_2CO_3). Aqueous NaOH only maintained a partial fibrous structure of Ch while saturated aqueous Na_2CO_3 improved neutralisation [17]. The proposed post-treatment of Ch performed in a 70/30 ethanol/1 potassium carbonate (M

K_2CO_3) ratio has allowed researchers to obtain pure Ch nanofibres with unprotonated amine groups (NH_2) and a preserved morphology [20, 22].

It is known that the solvent remnants in electrospun membranes could influence biological properties due to toxicity, and effective solvent removal is required before biomedical applications. In this work, aqueous 1 M Na_2CO_3 and 1 M NaOH and water/ethanol solutions were compared to fix Ch membranes obtained by electrospinning and removing solvents (TFA and DCM). Organic solvents are better dissolved in polar organic compounds than in water; hence, ethanol was used for this purpose. NaOH or Na_2CO_3 is better dissolved in water; hence, a water/ethanol solution (70% ethanol/30% aqueous solution) was used to dissolve NaOH or Na_2CO_3 in the water component and TFA/DCM in ethanol. The amount of ethanol should be higher than water to increase fast solvent evaporation and to decrease swelling of the Ch membrane. The various ethanol/aqueous solution ratios were compared, but only 70/30 was the most appropriate. The ideal method to fabricate cross-linked electrospun Ch membranes with biocompatibility and strong antimicrobial properties for medical application remains a relevant topic. The goal of the current research was to select the solution for the production of nanofibrous insoluble Ch membrane using various TFA/DCM solvent ratios suitable for biomedical application and tissue engineering. The structural, electronic, and optical properties, and swelling capacity of the prepared nanofibre membranes were studied with cell viability (resazurin reduction assay) and bacteriological assays (Kirby Bauer disk diffusion method and turbidimetric determination of bacterial growth).

2. Materials and Methods

2.1. Materials

Low-molecular-weight Ch powder (890,000 Da) was purchased from Glentham Life Sciences (Corsham, United Kingdom) CAS 9012-76-4. All other reagents – DCM (CAS 75-09-2), TFA (CAS 76-05-1), Na_2CO_3 (CAS 144-55-8), and NaOH (CAS 1310-73-2) – were purchased from Sigma-Aldrich (St. Louis, MO, USA).

2.2. Preparation of Ch Solutions

The 3.5 wt.% Ch solution was prepared by dissolving Ch powder in TFA/DCM at a volume ratio of 7:3 v/v (Solution 1) or 9:1 v/v (Solution 2) under magnetic stirring overnight at room temperature until a homogeneous solution was formed. Electrospinning of the obtained solutions was carried out no more than 12 h after their preparation. Before electrospinning, the solutions were kept at room temperature in the syringes for 30 min to remove air bubbles.

2.3. Electrospinning Ch Nanofibre Membranes

The electrospinning system used for fibre preparation consisted of a syringe pump, a high-voltage DC power supply generator (Linari Engineering s.r.l., Pisa, Italy), and a cylindrical rotating drum wrapped with aluminium foil (30 mm diameter, 120 mm length) with a controllable rotating speed from 0 to 3000 rpm (model RT-Collector Web, Linari Engineering s.r.l).

Ch solution was transferred into a 10 ml plastic syringe with a metallic bent needle (0.69 mm inner diameter). A syringe pump delivered the Ch solution to the needle tip at a pump rate of 5.0 ml/h. A 33 kV electric field was maintained between the two electrodes. The rotating speed was 1000 rpm. The collector was placed 15 cm from the needle tip. The deposition was performed at relative humidity of 35% and 23°C. Ch membranes were then peeled off the collector and dried under vacuum at 50°C for 12 h.

2.4. Neutralisation Treatments of Ch Nanofibre Membranes

To prevent Ch nanofibre membranes from dissolution in the aqueous medium, they were neutralised in different sodium-based solutions (NaOH and Na_2CO_3) [23]. The treatment was performed by neutralising each mat in 1 M NaOH and 1 M Na_2CO_3 (aqueous or 70% ethanol/30% aqueous solution, v/v) in a plastic 24-well plate for 24 h. After immersion, the membranes were repeatedly washed with distilled water and dried at ambient conditions for 1 day at room temperature. After treatment, the following samples were obtained: Solution 1 and Solution 2 with NaOH aqueous and NaOH-ethanol treatment, respectively, and Solution 1 and Solution 2 with Na_2CO_3 aqueous and Na_2CO_3-ethanol treatment, respectively.

2.5. Scanning Electron Microscopy (SEM)

Samples from each electrospun membrane (5 × 5 mm), placed on a metal plate, were covered with a carbon layer at the vacuum set-up VUP-5M (SELMI, Sumy, Ukraine). The morphology of fibres was observed by using a FEI Inspect S50B scanning electron microscope (FEI, Brno, Czech Republic) at an acceleration voltage of 10 kV. ImageJ software (National Institutes of Health, Bethesda, MD, USA) was used to analyse the fibre diameters by measuring 100 fibres chosen randomly from each specimen.

The parameter 'porous area fraction' was selected to describe the morphological structure of the membranes. The 'porous area fraction' is determined by the area of the pores divided by the total area of the investigated image region. The 'porous area fraction' does not correspond directly to a 'pore size' but rather to a 'local porosity' [24].

2.6. Fourier-Transform Infrared (FT-IR) Spectroscopy

FT-IR spectra of the samples were obtained with an FTIR spectrometer (Bruker Alpha II, USA) in the range of 500-3000 cm^{-1}. FTIR peaks were analysed using Origin software (OriginPro, version 9.5.1, Northampton, MA, USA).

2.7. Optical Properties

Photoluminescence (PL) spectra of Ch nanofibre membranes was measured by 300 nm LED, Thorlabs 2 mW output power (Thorlabs Inc, Ann Arbor, Michigan, USA), and Ocean optic HR4000 spectrometer (Ocean Optics, Dunedin, FL, USA).

2.8. Weight Loss and Swelling Capacity

The swelling capacity of the Ch membranes (15 × 15 mm) was tested by evaluating the weight difference between the swollen state in water at a neutral pH after 20 and 60 min and the final dried weight at room temperature. The average of three measurements of the wet swollen samples and the sizes of the dried specimens were used to determine the swelling ratio using Equation (1) [21, 22]:

$$SC\,(\%) = (Ws - Wd)/Wd \times 100\; SC\,(\%) = (Ws - Wd)/Wd \times 100 \qquad (1)$$

where Ws (g) is the weight of the swollen nanofibrous membrane and Wd (g) is the weight of the samples after drying at room temperature.

The percentage weight loss of the samples (15 × 15 mm) was calculated before and after immersion in phosphate-buffered saline (PBS). The membranes were incubated in PBS to simulate *in vitro* degradation conditions. Treated Ch membranes were soaked in PBS (pH 7.4) for 1 day, 3 days, 1 week, and 1 month. Then, the samples were rinsed with Milli-Q water and dried overnight at room temperature to remove the absorbed water. The

measurements were carried out three times each. The percentage weight loss of samples after immersion was calculated using Equation (2) [24]:

$$WL\ (\%) = (Wi - Wd)/Wi \times 100\ WL\ (\%) = (Wi - Wd)/Wi \times 100 \quad (2)$$

where Wd (g) is the weight of the sample in its dry state after submersion in PBS and Wi (g) is the initial weight of the sample in its dry state before submersion in PBS.

To assess the degradation trends of membranes, the morphology of the nanofibre membranes was studied by SEM. After 1 month, the samples were removed from the solution, rinsed with distilled water, and dried at 25°C. The membranes were sputter-coated with silver and assessed by SEM.

2.9. Cell Viability Study

Cell culture experiments were performed to access the biocompatibility of Ch membranes. Human bone osteosarcoma epithelial cells (the U2OS cell line) were grown in 75 cm² cell culture flasks under standard culture conditions of humidified air containing 5% carbon dioxide (CO_2) at 37°C with medium renewal every 2-3 days. Dulbecco's Modified Eagle Medium/nutrient mixture F-12 (DMEM/F-12) with L-glutamine was used, containing 100 units/ml penicillin, 100 µg/ml streptomycin, 2.5 µg/ml amphotericin B, and 10% foetal bovine serum. Ch membranes were cut (5 × 5 mm) and immersed in 70% ethanol for 30 min for sterilisation followed by five washes in PBS for 5 min each to eliminate any ethanol residual. After that, the samples were placed in a 24-well cell culture plate and immersed in PBS overnight. The next day, U2OS cells were seeded on samples at the density of 1×10^4 cells per well, and the culture medium was added. After 24 h, 10 µl (10% of the culture medium volume) of resazurin solution (0.15 mg/ml, pH 7.4) was added to each well. The plates were incubated for 4 h at 37°C in the dark. One hundred microlitres of medium from each well was transferred to another 96-well plate. The absorbance was measured using a Multiskan FC (Thermo Fisher Scientific, Waltham, MA, USA) plate reader at 570 and 600 nm. The resazurin reduction assay was repeated on days 3 and 6. Each sample was run in triplicate.

After the final day, samples were prepared for SEM and fluorescent 4′,6-diamidine-2′--phenylindole dihydrochloride (DAPI, Roche, Switzerland) staining. For SEM, the medium was removed from the membranes, which were then washed in room-temperature PBS to remove excess protein. For fixation, the membranes were immersed in 2.5% glutaraldehyde (in 0.1 M PBS) 2 × 40 min, followed by PBS washing (2 × 15 min). Dehydration was performed by immersing the samples in increasing alcohol concentrations (50%, 70%, 90%, and 96%) for 30 min at each concentration. After aspirating the 96% alcohol, the samples were immersed in 96% alcohol overnight. The alcohol was aspirated, and the samples were left on their plate uncovered overnight to allow the remaining ethanol to evaporate. For fluorescence microscopy, samples were washed in PBS twice and incubated with 1:35.000 DAPI in PBS for 2 min. After that, all samples were analysed with a fluorescence microscope (Axio Imager A1 microscope, Carl Zeiss, Germany) in the DAPI channel.

2.10. Antibacterial Activity Evaluation

The antibacterial properties were examined against gram-positive *Staphylococcus aureus* and gram-negative *Escherichia coli* bacteria obtained from Sumy State University's Bacteria Collection. Nanofibre samples were cut with a 0.5 cm diameter and sterilised with ultraviolet (UV) radiation at 254 nm for 1 h.

2.10.1. Antibacterial Resistance Assay

The inhibitory activity of Ch nanofibre membranes was evaluated via antibacterial resistance measurements using the Kirby Bauer disk diffusion method. The bacterial cultures were incubated in nutrient broth at 37°C for 24 h. The suspension concentration was adjusted to 1×10^5 colony-forming units (CFU)/ml ($5 \log_{10}$ CFU/mL). One hundred microlitre aliquots of a bacterial suspension were spread and dispersed with a sterile glass rod onto the Mueller-Hilton agar plates. Then, sterile Ch membranes (the same cell viability study sterilisation method was used) were deposited by sterile forceps on the surface of agar plates and incubated at 37°C for 48 h [25]. The dimensions of the zones of inhibition were determined in triplicate.

2.10.2. Time-Dependent Bacterial Growth Assay

A direct contact test was used based on the turbidimetric determination of bacterial growth in 96-well microtitre plates. Samples were placed into a sterile 24-well plastic plate containing bacterial suspension in the concentration of 1×10^5 CFU/mL for 2, 4, 6, and 8 h. Determination of the intensity of the opacity was performed via medium transmittance measurement on a Thermo Scientific Multiskan FC spectrophotometer at 595 nm [26]. The turbidity with microbial growth without the effect of the Ch membrane was used as the positive control. The negative control wells contained a sterile, microbe-free nutrient broth medium. The average absorbance values for each set of triplicate controls and samples were calculated.

After incubation in bacterial suspension, samples were prepared for SEM to estimate bacterial cell attachment, dissemination, and morphology on the Ch nanofibres. The sample preparation for SEM was similar to that described in Section 2.9.

2.11. Statistical Analysis

Statistical analysis was performed using SPSS software version 8.0 (SPSS Inc., Chicago, IL, USA). All experiments were conducted in triplicate. The results are expressed as mean ± standard deviation. One-way analysis of variance was used to determine the level of significance ($p < 0.05$ was defined as significant).

3. Results and Discussion

3.1. SEM

Scanning electron micrographs of the electrospun membranes prepared from a Ch solution with different TFA/DCM volume ratios are presented in Figure 1, section A. All samples were free of beads, indicating that the tested Ch electrospinning conditions provide sufficient chain entanglement for fibre formation. Zhang *et al.* [27] explained that the formation of small particles over the electrospun fibre surface is due to the presence of salts originating from Ch dissolution in TFA. These salts are commonly observed for higher polymer concentrations and TFA content in the Ch-TFA/DCM solvent solution. The surfaces of the membranes without neutralisation exhibit a regularity and uniformity resulting from the drying process. The average fibre diameters were 0.18 ± 0.009 μm and 0.2 ± 0.01 μm for Solution 1 and Solution 2, respectively. The 'porous area fraction' of the membrane made with Solution 1 (38.94% ± 5.6%) was higher than Solution 2 (5.4% ± 1.9%).

The average fibre diameter did not decrease significantly as the DCM content increased. On the other hand, there was a wider fibre size distribution as the TFA content in the solution increased. The membranes prepared from Solution 1 demonstrated a more uniform fibre size distribution (Figure 1, section B). The morphology and influence on

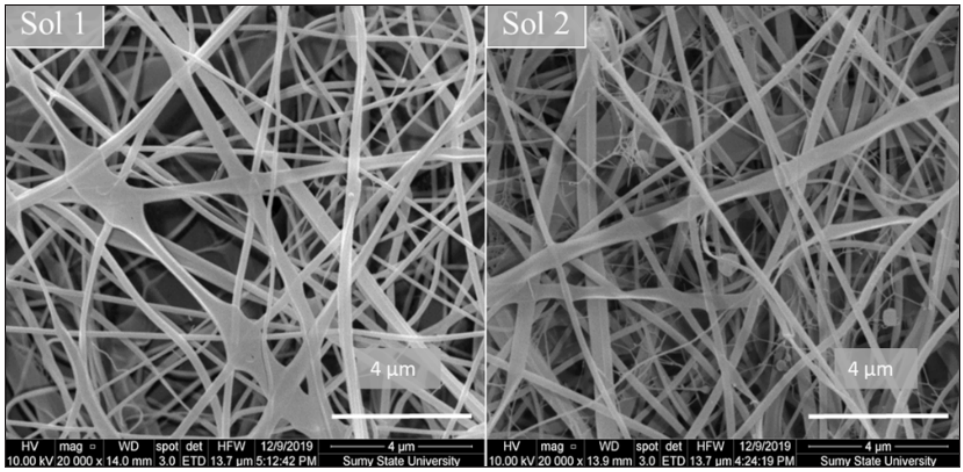

Figure 1 (section A). Scanning electron micrograph of as-spun chitosan membranes made with Solution 1 (TFA/DCM = 7:3) (A) and Solution 2 (TFA/DCM = 9:1) (B).

fibre size distribution in samples after alkaline treatment are summarised in Figure 1, section C. The nanofibrous membranes neutralised in aqueous Na_2CO_3 or Na_2CO_3-ethanol solutions did not preserve the nanofibrous structure, and there was a film-like structure. Therefore, it was impossible to characterise the fibre size for any membranes after Na_2CO_3 treatment. Traditional neutralisation with aqueous NaOH only maintained a partial fibrous structure. The fibre diameter of Solution 1 and Solution 2 membranes increased up to 0.52 ± 0.025 µm and 1.07 ± 0.048 µm due to partial swelling of protonated Ch at first contact with an aqueous solution. On the contrary, SEM confirmed the stability of the nanofibrous structures after treatment with aqueous NaOH-ethanol (70/30). The fibre diameter increased to 0.37 ± 0.015 µm and 0.3 ± 0.01 µm for Solution 1 and Solution 2 membranes, respectively. A previous study also indicated that washing Ch membranes increased nanofibre swelling without changing the fibre morphology [21].

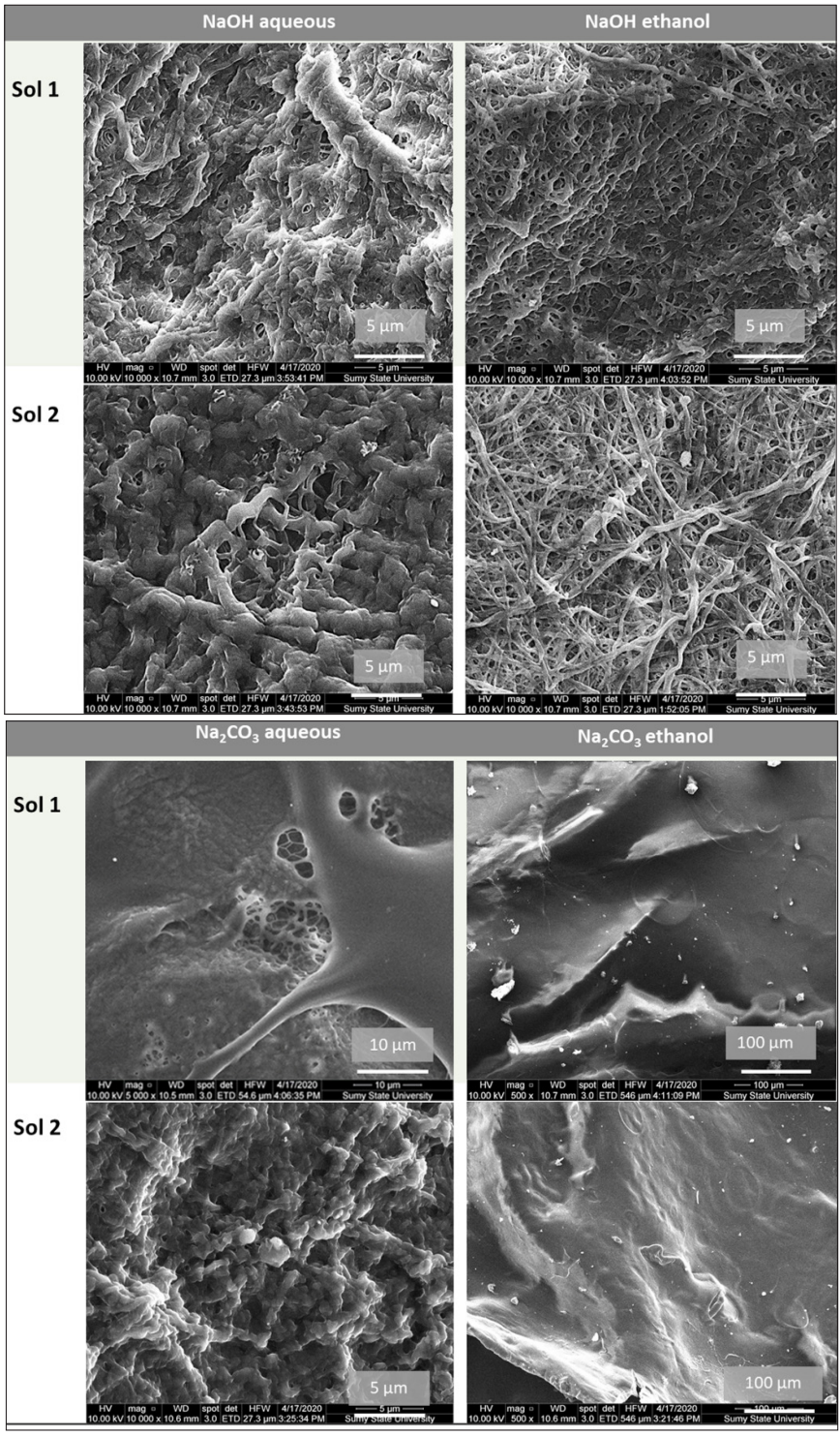

Figure 1 (section B). Scanning electron micrographs of chitosan membranes made with Solution 1 and Solution 2 after neutralisation in aqueous 1 M NaOH, aqueous 1 M Na_2CO_3, 1 M NaOH-ethanol, or 1 M Na_2CO_3-ethanol (70% ethanol/30% aqueous) solutions.

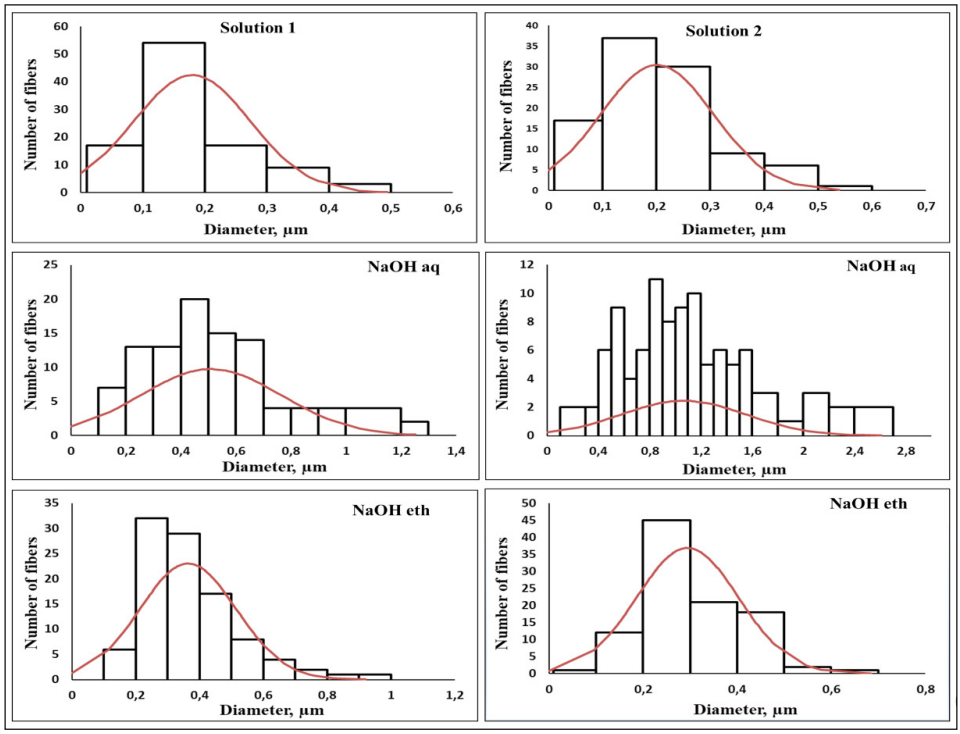

Figure 1 (section C). Fibre diameter distribution diagrams of chitosan membranes made with Solution 1 or Solution 2 before and after neutralisation with aqueous 1 M NaOH or 1 M NaOH-ethanol (70% ethanol/30% aqueous NaOH) solution. There are no fibre diameter diagrams after neutralisation in Na_2CO_3 because the fibres dissolved and a film-like structure formed.

3.2. FT-IR

FTIR was used to assess the chemical modifications of the Ch chains due to dissolution in TFA/DCM and subsequent neutralisation [18]. FTIR spectra of as-deposited and post-treated samples are presented in Figure 2. There are characteristic absorption peaks of Ch at 616, 664, and 897 cm^{-1}, corresponding to O-H out of the plane, N-H out of the plane, and pyranose ring stretching, respectively. The presence of three absorption peaks around 720-840 cm^{-1} could indicate the TFA in Ch nanofibres. The absorption peaks of the Ch membrane observed at 1530 and 1667 cm^{-1} correspond to the stretching of the protonated amino ($-NH_3^+$) groups [28]. The amide I peak at 1654 cm^{-1} is attributed to the out-of-plane bending vibration of the C=O group. The sharp, low-intensity peak at 1550 cm^{-1} is attributed to the amide II peak, where the in-plane bending vibration of N-H and the stretching vibration of the C-N bond overlap. The amide III peak at 1386 cm^{-1} is attributed to the overlapping of the in-plane-scissoring vibration of the N-H bond and the stretching vibration of the C-N bond. The symmetric and asymmetric CH_2 stretching vibrations can be seen at 2886 cm^{-1}, attributed to the stretching vibration of the C-H bond in the pyranose ring. The peak at 903 cm^{-1} is characteristic of the stretching vibration of C-O-C bonds in the glucosamine ring and the saccharide ring's out-of-plane bending vibration [29]. Absorption peaks at 1035-1080 cm^{-1} and 1120-1200 cm^{-1} correspond to C-OH stretching vibration and C-O-C asymmetric bending vibration, respectively. Absorption peaks

at 2885 and 3447 cm^{-1} correspond to CH_3 symmetric stretch and N-H/O-H out-of-plane stretching vibration, respectively [30].

Neutralisation of the samples changed the electronic structure of the Ch membranes prepared by either Solution 1 or Solution 2. Post-treatment was applied to fix CS fibres after solvent removal. After post-treatment of CS fibres with Na_2CO_3-ethanol or NaOH-ethanol solutions, obtained from Solution 2 (Figure 2B) or Solution 1 (Figure 2A), there is suppression of peaks in the range of 600-900 cm^{-1} (N-H out of the plane and pyranose ring stretching vibration), 1000-1060 cm^{-1} (C-OH stretching vibration), 1120-1200 cm^{-1} (C-O-C asymmetric bending vibration), 1530, and 1667 cm^{-1} (stretching of the protonated amino [-NH_3^+] groups). Meanwhile, after post-treatment of CS fibres, obtained from Solution 2 with aqueous Na_2CO_3, all peaks of as-deposited CS remain unchanged (Figure 2B). After post-treatment of CS fibres obtained from Solution 1, peaks at 616, 664, and 897 cm^{-1}, corresponding to O-H out of the plane, N-H out of the plane, and pyranose ring stretching vibrations are suppressed, respectively. The amide I peak at 1654 cm^{-1} (the out-of-plane bending vibration of the C=O group) is also suppressed (Figure 2A).

Analysis of FTIR spectra after post-treatment of CS fibres, obtained from Solution 2 (Figure 2B) and Solution 1 (Figure 2A) with neutralisation in aqueous NaOH, shows suppression of peaks in the range of 600-900 cm^{-1} (O-H out of the plane, N-H out of the plane, and pyranose ring stretching vibrations). The absorption peaks at 1530 and 1667 cm^{-1}, corresponding to the stretching of the protonated amino (-NH_3^+) groups, are also suppressed. The intensity of mentioned peaks is decreased for Solution 1. The mentioned treatments remove TFA traces; reduce the NH_3^+ concentration; and change stretching modes of C-C, C-O, and C-OH vibrations. The post-treatment retains CH_3 symmetric stretching and N-H/O-H stretching vibrations.

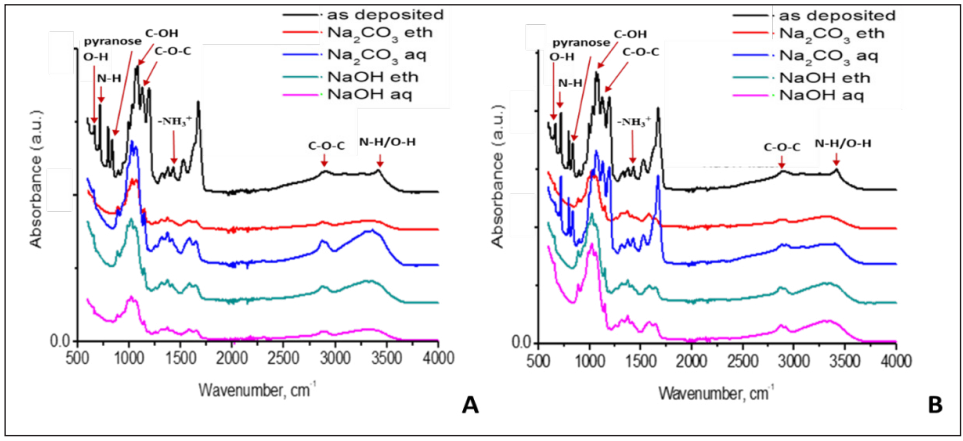

Figure 2. Fourier-transform infrared spectra of chitosan membranes made with Solution 1 (A) or Solution 2 (B).

Some mechanisms explain the structural and chemical features of the Ch membranes made with different solutions. TFA can dissolve the polymer by forming salts that destroy the strong interactions between Ch molecules [17]. The salt formation occurs between TFA and the amino groups along the Ch chain after the following sequential steps: first, protonation of amine groups (-NH_2) along the Ch chain; second, ionic interaction between protonated amine groups (-NH_3^+) and then the formation of trifluoroacetate anions.

The salts are soluble in aqueous media [28]. Ch turns into a polyelectrolyte when it is dissolved in acidic media. Its free amino groups become protonated, and repulsive forces appear between these ionic groups. Hasegawa *et al.* [28] studied the dissolution of Ch in TFA. They concluded that dissolution occurs due to the formation of amine salts at the amine groups of C_2 (second carbon atom on the Ch molecule) with TFA and noted that no trifluoroacetylation occurs at the hydroxyl groups of Ch. TFA decreases the boiling point and surface tension, making it a suitable solvent for electrospinning. It has also been shown that the addition of a small amount of DCM facilitates electrospinning of Ch because it further reduces the boiling point of the solvent system and also reduces the extreme charge density originated by the TFA. For these reasons, a TFA/DCM solvent system was selected in the present study to produce Ch blend solutions and electrospun them into nanofibrous structures [28].

3.3. Optical Properties

The PL spectra of the measured samples are shown in Figure 3. As prepared, the Ch samples have a broad emission centred at 390 nm. The observed emission is related to the π*-π transition [31, 32]. Treatment with Na_2CO_3 or NaOH quenched the PL intensities for both samples. The role of pH in Ch properties has been reported [33, 34]: alkaline treatment ~~with a pH <4~~ results in the formation of hydroxyl groups on the Ch surface. Treatment of the Ch nanostructures with sodium tripolyphosphate results in phosphate anions on the Ch surface [33]. The results of pH analysis of gelatine-Ch blends showed PL intensity in alkaline solutions was reduced due to the formation of hydroxyl groups and hydrogen bonds [34]. Therefore, the obtained spectra of the post-treated Ch could show reduced emission due to forming of hydroxyl and anion groups on the surface.

However, FTIR analysis showed suppression of the fundamental vibration bands of Ch after post-treatment. There are no new vibrations related to hydroxyl groups. Therefore, the main mechanism of PL quenching is connected to changes in π*-π transition after post-treatment. The FTIR data showed a significant reduction in C-C vibrations, which correlates with PL quenching in post-treated samples.

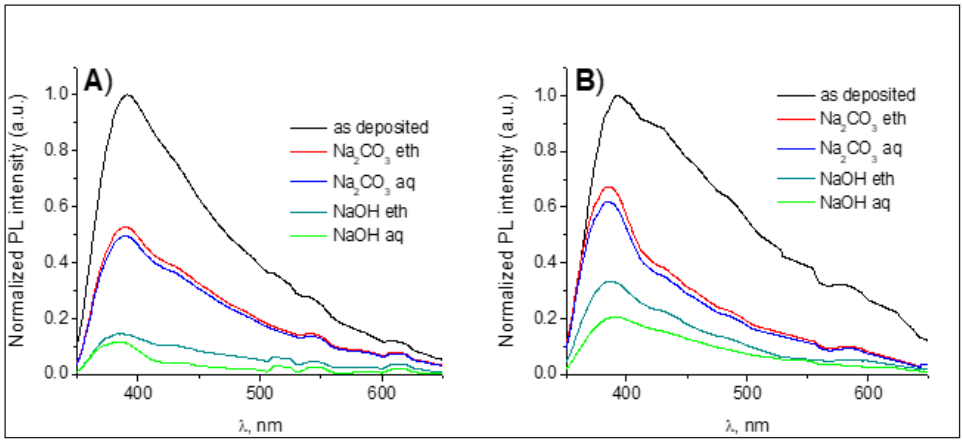

Figure 3. Photoluminescence spectra of as-deposited and alkaline-treated electrospun chitosan membranes made with Solution 1 (A) or Solution 2 (B).

3.4. Weight Loss and Swelling Capacity

The swelling capacity of alkaline-treated Ch membranes prepared in 9:1 TFA/DCM was 2 and 1.5 times higher than that of the nanofibres created in 7:3 TFA/CDM system after 20 and 60 min submersion in PBS, respectively (Figure 4A). Weight loss was significantly higher for membranes made with Solution 2 than for Solution 1 ($p \leq 0.05$) on days 1 and 3 of the experiment. However, the weight loss of membranes made with Solution 1 was significantly higher after 1 week and 1 month of submersion in PBS (Figure 4B). The degradation of Ch polymers occurs by hydrolysis and oxidation. The degradation by hydrolytic mechanism involves the reaction of weak bonds in the polymer with water. The rate of degradation depends on the accessibility of water into the polymer matrix rather than the intrinsic rate of ester cleavage [29].

In the present research, after neutralisation in NaOH-ethanol, fibres of electrospun Ch membranes maintained their structure even after continuous submersion in PBS (pH 7.4) or distilled water for 1 month. The long immersion in PBS influenced the general nanofibrous structure and caused membrane disintegration (Figure 4C and 4D). After 1 month, there was pore collapsing, the formation of large holes, fibre fusion, and the appearance of microcracks.

Electrospun Ch membranes treated with aqueous Na_2CO_3 demonstrated different degradation characteristics depending on the co-solvent system ratio. The nanofibrous membranes fabricated from the 9:1 TFA/DCM Ch solution possessed an increase in swelling capacity and weight loss. These differences could be explained by the TFA removal and consequently higher weight reduction within neutralisation and immersion into PBS within the initial time points of the experiment.

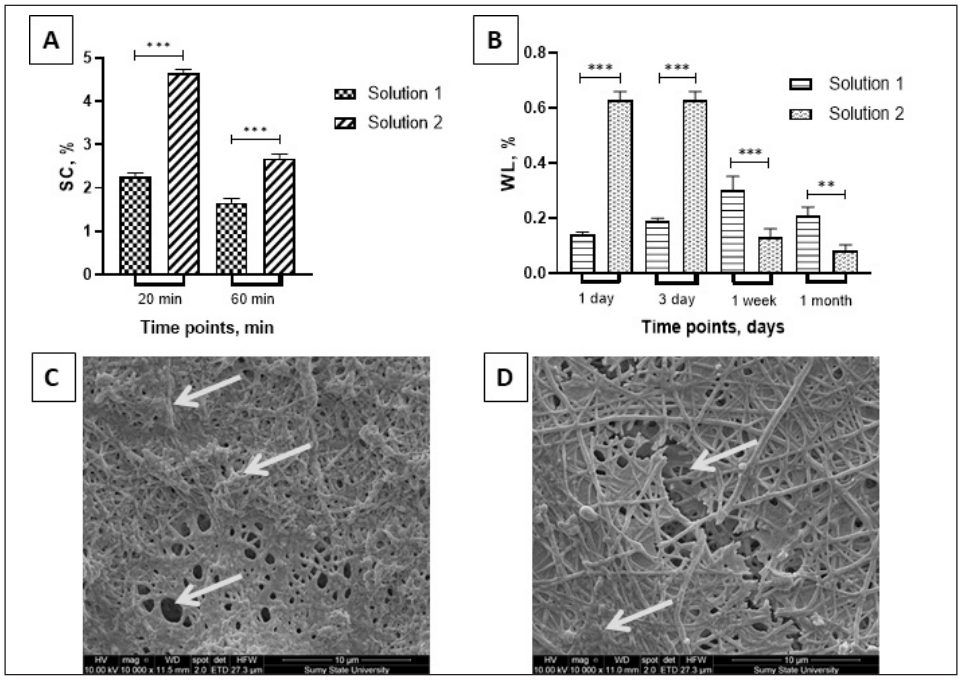

Figure 4. The degradation kinetics (swelling capacity [A] and weight loss [B]) of the post-neutralised electrospun chitosan nanofibrous membranes with different trifluoroacetic acid/dichloromethane ratios and scanning electron micrographs of chitosan membranes in phosphate-buffered saline (C and D). Arrows demonstrate mat defects.

3.5. Cell Viability Study

It is important to note that all membranes retained their structure during the 6 days of incubation, except for the sample treated with 1 M Na_2CO_3. The cells remained viable during the observation period. The attachment rate did not differ significantly among the groups and reached around 50% of resazurin reduction. Membranes made with Solution 2 demonstrated appropriate cell proliferation on days 3 and 6 with no significant difference between the neutralisation methods (Figure 5A). The cell proliferation in membranes made with Solution 1 strongly depended on the neutralisation method (Figure 5B). On both days 3 and 6, ethanol-treated membranes demonstrate a significantly lower resazurin reduction rate than non-treated membranes and membranes treated with aqueous NaOH or Na_2CO_3. Due to the larger pore area of the membrane made with Solution 1, ethanol could diffuse to media and affect cell growth.

SEM of Ch membranes on day 6 demonstrates uniform cell distribution over the sample surface. The U2OS cells present an elongated morphology with short and lengthy processes in contact with nanofibres (Figure 5C). At high magnification (Figure 5D), cells deeply integrated with electrospun nanofibres cover the cell wall, indicating cell migration within membrane pores. Fluorescent DAPI staining demonstrated that cells completely covered the membrane surface in all membranes made with Solution 1, while membranes made with Solution 2 and neutralised in NaOH-ethanol or Na_2CO_3-ethanol had significantly fewer cells.

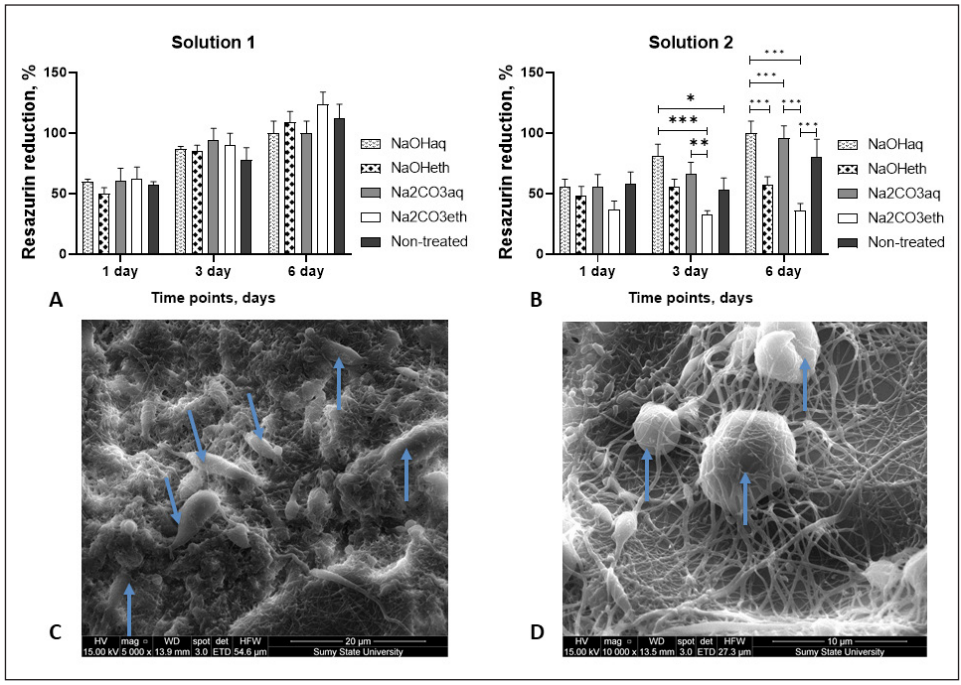

Figure 5. Resazurin reduction assay with U2OS cells seeded on chitosan electrospun membrane made with Solution 1 (A) or Solution 2 (B). Panels C and D demonstrate the U2OS cell distribution over the chitosan electrospun membrane 6 days after cell seeding. Blue arrows show cells.

3.6. Antibacterial Activity

The antimicrobial resistance of the samples measured by the Kirby Bauer disk diffusion method is summarised in Table 1. Bacteria did not grow within the membranes, and the inhibition zones were 5-10 mm. The nanofibrous membranes prepared from Solution 1 or Solution 2 demonstrated comparable resistance to microbial penetration.

Table 1. Inhibition zones of chitosan samples against *Escherichia coli* and *Staphylococcus aureus*.

Alkaline treatments		Inhibition zone diameter [mm]			
		S. aureus		*E. coli*	
		Solution 1	Solution 2	Solution 1	Solution 2
Non-treated sample	1	8 ± 0.1	5 ± 0.1	7 ± 0.1	5 ± 0.1
NaOH aqueous	2	5 ± 0.1	7 ± 0.1	7 ± 0.2	6 ± 0.2
NaOH ethanol	3	7 ± 0.1	8 ± 0.1	7 ± 0.2	6 ± 0.1
Na_2CO_3 aqueous	4	8 ± 0.2	5 ± 0.1	8 ± 0.3	8 ± 0.3
Na_2CO_3 ethanol	5	10 ± 0.3	5 ± 0.1	5 ± 0.1	10 ± 0.3

Note. The data are presented as the mean ± standard deviation.

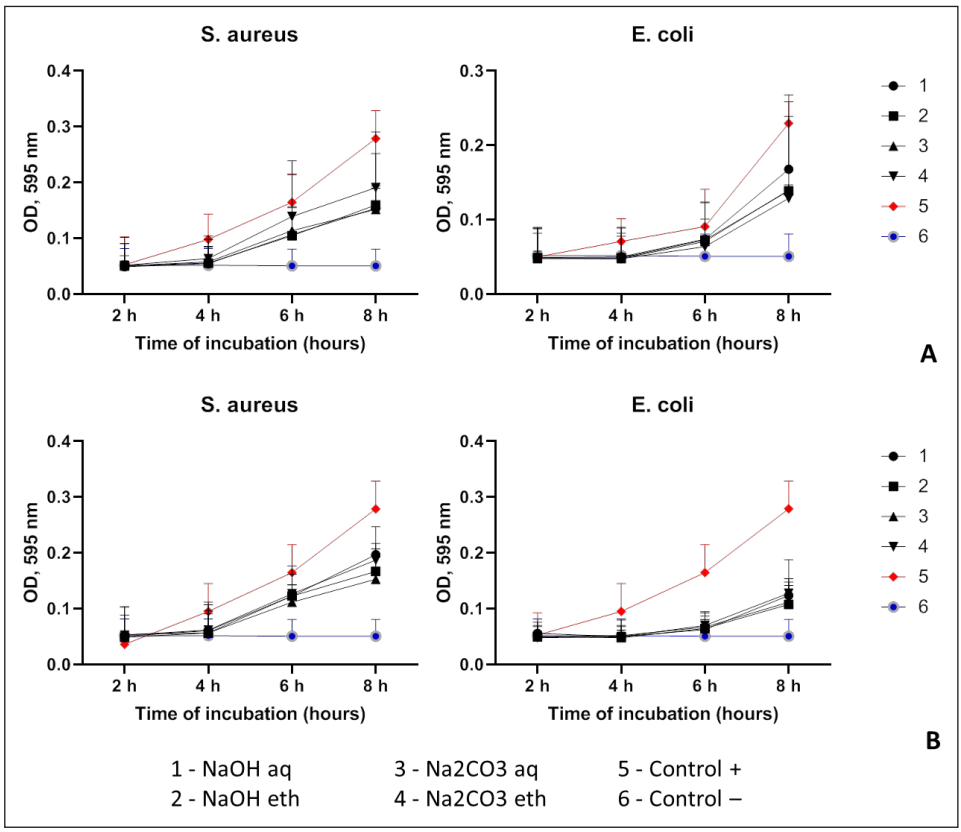

Figure 6. The optical density at 595 nm of the medium with *Escherichia coli* and *Staphylococcus aureus* after cultivation with chitosan membranes fabricated from Solution 1 (A) or Solution 2 (B).

The intensity of the turbidity caused by microbial growth revealed the penetration of microorganisms through the membranes [35]. All of the tested membranes could inhibit the penetration of bacteria into the nutrient medium (Figure 6). This phenomenon can be explained by the chelating effect of Ch, which affects bacterial growth and homeostasis [36]. The spectrophotometric growth curves revealed fewer bacterial cells after co-cultivation with Ch membranes than in positive control wells at the corresponding time point of the test (lower transmittance of the medium represents a higher number of microbial cells). Hence, nanofibrous mats made with both solutions could constrain the growth of both gram-positive and gram-negative microorganisms without dependence on the type of treatment. Nevertheless, *E. coli* showed greater sensitivity to the samples. Moreover, membranes prepared with Solution 1 inhibited bacterial growth more efficiently than samples prepared with Solution 2.

SEM demonstrated that microorganisms grow on the membrane surface and do not penetrate inside pores (Figure 7). NH_3^+ groups of Ch can bind with negatively charged gram-negative bacteria and inhibit their proliferation [37]. In addition, Ch can form

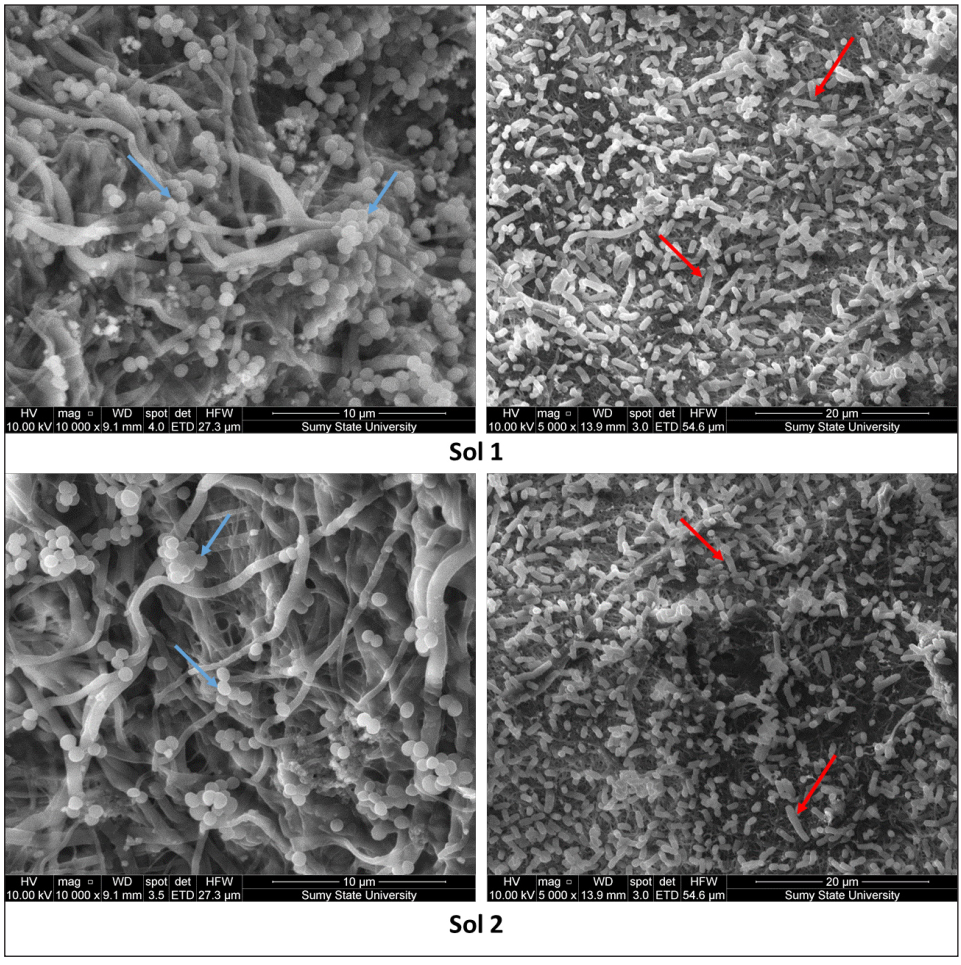

Figure 7. Scanning electron micrographs of *Staphylococcus aureus* (blue arrows) and *Escherichia coli* (red arrows) growth on chitosan nanofibre membranes treated with aqueous Na_2CO_3 after 8 hours of co-cultivation.

a polymer envelope of gram-positive microorganisms, preventing cell exchanges and absorbing nutrients [38]. Besides, lipoteichoic acid (LTA) of gram-positive bacteria could link the bacterial membrane and Ch chain that inhibit bacteria proliferation [39].

4. Conclusions

New Ch membranes prepared with two TFA/DCM ratios (7:3 and 9:1) were fabricated by conventional electrospinning followed by treatment with aqueous 1 M NaOH, aqueous 1 M Na_2CO_3, NaOH-ethanol, or Na_2CO_3-ethanol solutions. Ch membranes made with 7:3 TFA/DCM demonstrated significantly higher porosity with a more uniform fibre size distribution compared with Ch membranes made with 9:1 TFA/DCM. The nanofibrous membranes neutralised in aqueous Na_2CO_3 failed to preserve the nanofibrous structure by forming a film-like structure. In contrast, NaOH-ethanol (70/30) post-treatment preserved the nanofibrous structure. Ethanol-Na_2CO_3 neutralisation did not maintain the nanofibrous structure, and only aqueous NaOH maintained a partial fibrous structure. In addition to structural stability, NaOH-ethanol neutralisation maintained membrane resistance in PBS and distilled water over 1 month. All variants of membranes (as-fabricated and after neutralisation) supported cell adhesion and proliferation during a 6-day period, but ethanol treatment of Ch membranes made from 9:1 TFA/DCM exhibited reduced cell growth. Ch membranes made from 7:3 TFA/DCM exhibited biocompatibility alongside moderate and more efficacious antibacterial activity against *S. aureus* and *E. coli*. To summarise experimental findings, Ch membranes fabricated using 7:3 TFA/DCM and then neutralised in 70% ethanol/30% aqueous solution exhibit potential for biomedical application in regenerative medicine and as tissue-engineering scaffolds.

5. Acknowledgments

This research was funded by a grant from the Ministry of Education and Science of Ukraine (0120U101972) and H2020-RISE project 777926. FT-IR and FL measurements were made during the Latvian Governmental Scholarship visit of V.K. and V.H. to the University of Latvia.

6. Disclosure

The authors report no conflicts of interest in this work. Data are available by request.

7. References

[1] Rasouli R, Barhoum A, Bechelany M, Dufresne A; (2019) Nanofibers for biomedical and healthcare applications, Macromol Biosci 19(2). **DOI**:10.1002/mabi.201800256

[2] Contreras-Cáceres R, Cabeza L, Perazzoli G, Díaz A, López-Romero JM, Melguizo C, Prados J; (2019) Electrospun nanofibers: recent applications in drug delivery and cancer therapy. Nanomaterials 9(4). **DOI**:10.3390/nano9040656

[3] Shalumon KT, Binulal NS., Selvamurugan N, Nair SV, Menon D, Furuike T, Tamura H, Jayakumar R; (2009) Electrospinning of carboxymethyl chitin/poly(vinyl alcohol) nanofibrous scaffolds for tissue engineering applications. Carbohydr Polym 77(4), 863-869. **DOI**:10.1016/j.carbpol.2009.03.009

[4] Prabaharan M; (2015) Chitosan-based nanoparticles for tumor-targeted drug delivery. Int J Biol Macromol 72, 1313-1322. **DOI**:10.1016/j.ijbiomac.2014.10.052

[5] Du H, Liu M, Yang X, Zhai G; (2015) The design of pH-sensitive chitosan-based formulations for gastrointestinal delivery. Drug Discov Today 20(8), 1004-1011. **DOI**:10.1016/j.drudis.2015.03.002

[6] Sun K, Li ZH; (2011) Preparations, properties and applications of chitosan based nanofibers fabricated by electrospinning. Express Polym Lett 5(4), 342-361. **DOI**:10.3144/expresspolymlett.2011.34

[7] Nayak R; (2017) Experimental: melt electrospinning**.** Springer, Cham, 41-54.

[8] Pasricha R, Sachdev D; (2017) Biological characterization of nanofiber composites. In: Ramalingam M, Ramakrishna S (eds), Nanofiber composites for biomedical applications. Woodhead Publishing, Cambridge, 157-196.

[9] Ding B, Wang X, Yu J (eds); (2018) Electrospinning: nanofabrication and applications. Elsevier, Amsterdam.

[10] Rasouli R, Barhoum A, Bechelany M, Dufresne A (2019) Nanofibers for biomedical and healthcare applications. Macromol Biosci 19(2). **DOI**:10.1002/mabi.201800256

[11] Ngo DH, Vo TS, Ngo DN, Kang KH, Je JY, Pham HND, Byun HG, Kim SK; (2015) Biological effects of chitosan and its derivatives, Food Hydrocolloids 51. **DOI**:10.1016/j.foodhyd.2015.05.023

[12] Abrigo M, McArthur SL, Kingshott P; (2014) Electrospun nanofibers as dressings for chronic wound care: Advances, challenges, and future prospects. Macromol Biosci 14(6), 772-792. **DOI**:10.1002/mabi.201300561

[13] Deineka V, Sulaieva O, Pernakov M, Korniienko V, Husak Y, Yanovska A, Yusupova A, Tkachenko Y, Kalinkevich O, Zlatska A, Pogorielov M; (2021) Hemostatic and Tissue regeneration performance of novel electrospun chitosan-based materials**.** Biomedicines 9(6), 588. **DOI**:10.3390/biomedicines9060588

[14] Klossner RR, Queen HA, Coughlin AJ, Krause WE; (2008) Correlation of chitosan's rheological properties and its ability to electrospin.Biomacromolecules 9(10), 2947-2953. **DOI**:10.1021/bm800738u

[15] Deineka V, Sulaieva O, Pernakov N, Radwan-Pragłowska J, Janus L, Korniienko V, Husak Y, Yanovska A, Liubchak I, Yusupova A, Piątkowski M, Zlatska A, Pogorielov M; (2021) Hemostatic performance and biocompatibility of chitosan-based agents in experimental parenchymal bleeding. Mater Sci Eng C 120. **DOI**:10.1016/j.msec.2020.111740

[16] Sencadas V, Correia DM, Areias A, Botelho G, Fonseca AM, Neves IC, Gomez Ribelles JL, Lanceros Mendez S; (2012) Determination of the parameters affecting electrospun chitosan fiber size distribution and morphology. Carbohydr Polym 87(2), 1295-1301. **DOI**:10.1016/j.carbpol.2011.09.017

[17] Jayakumar R, SV, Furuike T, and Tamur H; (2010) Perspectives of chitin and chitosan nanofibrous scaffolds in tissue engineering. In: Eberli D (ed), Tissue Engineering, InTech Open, London. **DOI**:10.5772/8593

[18] Sencadas V, Correia DM, Ribeiro C, Moreira S, Botelho G, Gómez Ribelles JL, & Lanceros-Mendez S; (2012) Physical-chemical properties of cross-linked chitosan electrospun fiber mats. Polym Test 31(8), 1062-1069. **DOI**:10.1016/j.polymertesting.2012.07.010

[19] Huang Y, Onyeri S, Siewe M, Moshfeghian A, Madihally SV; (2005) In vitro characterization of chitosan-gelatin scaffolds for tissue engineering. Biomaterials 26(36), 7616-7627. **DOI**:10.1016/j.biomaterials.2005.05.036

[20] Qing H, Qiang A, Yandao G, Xiufang Z; (2011) Preparation of chitosan films using different neutralizing solutions to improve endothelial cell compatibility. J Mater Sci Mater Med 22, 2791-2802.

[21] Sangsanoh P, Supaphol P (2006) Stability improvement of electrospun chitosan nanofibrous membranes in neutral or weak basic aqueous solutions. Biomacromolecules 7(10), 2710-2714. **DOI**:10.1021/bm060286l

[22] Nitti P, Gallo N, Natta L, Scalera F, Palazzo B, Sannino A, Gervaso F; (2018) Influence of nanofiber orientation on morphological and mechanical properties of electrospun chitosan mats. J Healthc Eng 2018. **DOI**:10.1155/2018/3651480

[23] Phan DN, Lee H, Huang B, Mukai Y, Kim IS; (2019) Fabrication of electrospun chitosan/cellulose nanofibers having adsorption property with enhanced mechanical property. Cellulose 26(3), 1781-1793. **DOI**:10.1007/s10570-018-2169-5.

[24] Ziel R, Haus A, Tulke A; (2008) Quantification of the pore size distribution (porosity profiles) in microfiltration membranes by SEM, TEM and computer image analysis. J Memb Sci 323(2), 241-246. **DOI**:10.1016/j.memsci.2008.05.057

[25] Cremar L, Gutierrez J, Martinez J, Materon L, Gilkerson R, Xu F, Lozano K; (2018) Development of antimicrobial chitosan based nanofiber dressings for wound healing applications. Nanomedicine J 5(1), 6-14. **DOI**:10.22038/nmj.2018.05.002

[26] Lin B, Luo Y, Teng Z, Zhang B, Zhou B, Wang Q; (2015) Development of silver/titanium dioxide/chitosan adipate nanocomposite as an antibacterial coating for fruit storage. LWT 63(2), 1206-1213. **DOI**:10.1016/j.lwt.2015.04.049

[27] Zhang C, Yuan X, Wu L, Han Y, Sheng J; (2005) Study on morphology of electrospun poly(vinyl alcohol) mats. Eur Polym J 41(3), 423-432. **DOI**:10.1016/j.eurpolymj.2004.10.027

[28] Cheah WY, Show PL, Ng IS, Lin GY, Chiu CY, Chang YK; (2019) Antibacterial activity of quaternized chitosan modified nanofiber membrane. Int J Biol Macromol 126, 569-577. **DOI**:10.1016/j.ijbiomac.2018.12.193

[29] Dostert KH, O'Brien CP, Liu W, Riedel W, Savara A, Tkatchenko A, Schauermann, S, Freund HJ; (2016) Adsorption of isophorone and trimethyl-cyclohexanone on Pd(111): a combination of infrared reflection absorption spectroscopy and density functional theory studies. Surf Sci 650, 149-160. **DOI**:10.1016/j.susc.2016.01.026

[30] Vörös-Horváth B, Živković P, Bánfai K, Bóvári-Biri J, Pongrácz J, Bálint G, Pál S, Széchenyi A; (2022) Preparation and characterization of ACE2 receptor inhibitor-loaded chitosan hydrogels for nasal formulation to reduce the risk of COVID-19 viral infection. ACS Omega 7(4), 3240-3253. **DOI**:10.1021/acsomega.1c05149

[31] Geng Z, Zhang H, Xiong Q, Zhang Y, Zhao H, Wang g; (2015) A fluorescent chitosan hydrogel detection platform for the sensitive and selective determination of trace mercury(II) in water. J Mater Chem A 3(38), 19455-19460. **DOI**:10.1039/c5ta05610a

[32] Anas NAA, Fen YW, Omar NAS, Ramdzan NSM, Daniyal W. M. E. M. M., Saleviter S, Zainudin AA.; (2019) Optical properties of chitosan/hydroxyl-functionalized graphene quantum dots thin film for potential optical detection of ferric (III) ion. Opt Laser Technol 120. **DOI**:10.1016/j.optlastec.2019.105724

[33] Moeini A, Cimmino A, Dal Poggetto G, Di Biase M, Evidente A, Masi M, Lavermicocca P, Valerio F, Leone A, Santagata G, Malinconico M; (2018) Effect of pH and TPP concentration on chemico-physical properties, release kinetics and antifungal activity of Chitosan-TPP-Ungeremine microbeads. Carbohydr Polym 195, 631-641. **DOI**:10.1016/j.carbpol.2018.05.005

[34] Mi FL; (2005) Synthesis and characterization of a novel chitosan-gelatin bioconjugate with fluorescence emission. Biomacromolecules 6(2), 975-987. **DOI**:10.1021/bm049335p

[35] Abbaspour M, Makhmalzadeh BS, Rezaee B, Shoja S, Ahangari Z; (2015) Evaluation of the antimicrobial effect of chitosan/polyvinyl alcohol electrospun nanofibers containing mafenide acetate. Jundishapur J Microbiol 8(10), 24239. **DOI**:10.5812/jjm.24239

[36] Arkoun M, Daigle F, Heuzey MC, Ajji A; (2017) Mechanism of action of electrospun chitosan-based nanofibers against meat spoilage and pathogenic bacteria. Molecules 22(4), 585. **DOI**:10.3390/molecules22040585

[37] Raafat D, Sahl HG; (2009) Chitosan and its antimicrobial potential - a critical literature survey. Microb Biotechnol 2(2). 186-201. **DOI**:10.1111/j.1751-7915.2008.00080.x

[38] Zheng LY, Zhu JF; (2003) Study on antimicrobial activity of chitosan with different molecular weights. Carbohydr Polym 54(4), 527-530. **DOI**:10.1016/j.carbpol.2003.07.009

[39] Raafat D, Von Bargen K, Haas A, Sahl HG; (2008) Insights into the mode of action of chitosan as an antibacterial compound. Appl Environ Microbiol 74(12), 3764-3773. **DOI**:10.1128/AEM.00453-08